A Reliable and Efficient Procedure for Oscillator PPV Computation, With Phase Noise Macromodeling Applications

Alper Demir, *Member, IEEE,* and Jaijeet Roychowdhury, *Member, IEEE*

***Abstract*—The main effort in oscillator phase noise calculation and macromodeling lies in computing a vector function called the perturbation projection vector (PPV). Current techniques for PPV calculation use time-domain numerics to generate the system's monodromy matrix, followed by full or partial eigenanalysis. We present superior methods that find the PPV using only a single linear solution of the oscillator's time- or frequency-domain steady-state Jacobian matrix. The new methods are better suited for implementation in existing tools with harmonic balance or shooting capabilities (especially those incorporating "fast" variants), and can also be more accurate than explicit eigenanalysis. A key advantage is that they dispense with the need to select the correct one eigenfunction from amongst a potentially large set of choices, an issue that explicit eigencalculation-based methods have to face. We illustrate the new methods in detail using LC and ring oscillators.**

***Index Terms*—Eigenvalues and eigenfunctions, iterative methods, oscillator noise, phase jitter, phase noise, reduced-order systems, timing jitter.**

I. Introduction

AN IMPORTANT consideration during the design of communication systems is the phase noise performance of oscillators. Phase noise corrupts spectral purity and generates large power content in a continuous spread of frequencies around the desired oscillator tone, thus, contributing to adjacent channel interference. In clocked circuits, phase noise manifests itself as timing jitter, which leads to synchronization inaccuracies and eventually degrades system performance and bit error rate.

During system and circuit design, the usual procedure is to first estimate the phase noise or jitter of an oscillator, and to use this phase noise figure in an abstract representation of the oscillator. For example, it can be useful to represent an oscillator or a voltage-controlled oscillator as depicted in Fig. 1, i.e., as a time-domain Simulink, MATLAB, or AHDL model that produces as output a phase that contains a random component representing phase noise/jitter. The center frequency can be found easily from a steady-state solution of the oscillator. Characterization of the random phase noise or jitter component is more involved, and a simple, reliable, easy-to-implement procedure has been lacking.

Manuscript received May 30, 2002; revised October 1, 2002. This paper was recommended by Guest Editor G. Gielen.

A. Demir is with Koç University, 34450 Istanbul, Turkey.

J. Roychowdhury is with the University of Minnesota, Minneapolis, MN 55455 USA. (e-mail: jr@ece.umn.edu)

Digital Object Identifier 10.1109/TCAD.2002.806599

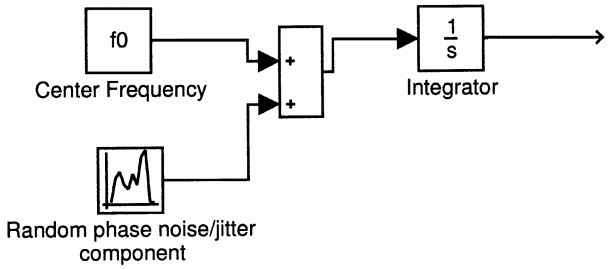

Fig. 1. Simple phase macromodel for oscillator.

Indeed, only recently has a rigorous understanding of the phase noise phenomenon in oscillators been developed [3], [4], despite long-standing interest in the problem.[1] A central conclusion of this new understanding is that the phase noise or jitter can be captured by a single scalar constant c, a statistical quantity representing the variance of the per cycle jitter in the oscillator. In fact, knowledge of c suffices to complete the macromodel in Fig. 1.

The per cycle jitter c depends not only on the noise generators in the oscillator, but also on a periodic vector function $v_1(t)$, termed the *perturbation projection vector* or *PPV*. c is given by, e.g.,

$$c = \frac{1}{T}\int_0^T v_1^T(\tau)B(x_s(\tau))B^T(x_s(\tau))v_1(\tau)\,d\tau \qquad (1)$$

where T is the period and x_s the steady-state solution of the unperturbed oscillator [4], while B encapsulates the noise contributions and bias-dependent noise modulations of the elemental device noise sources. The PPV can be intuitively thought of as the sensitivity of the per cycle jitter variance to current perturbations at the nodes of the oscillator. Calculating the PPV is the primary nontrivial step in finding c (hence in forming an oscillator phase noise macromodel).

In prior work [4], we presented a PPV calculation technique that we will term the *monodromy matrix method*. This method computes the state-transition (or *monodromy*) matrix of the linearized oscillator's adjoint differential equations by reverse time-domain numerical integration. Eigendecomposition of the monodromy matrix to find the eigenpair of the oscillatory mode[2] yields the PPV.

[1] A varied and extensive literature, developed over many decades, exists on the phase noise problem. We do not provide a review of prior work here as it is not central to our contribution, but we refer the interested reader to, e.g., [4], [6].

[2] Corresponding to eigenvalue 1, existence of which is guaranteed by Floquet analysis of orbitally stable oscillators (see e.g., [5]).

The monodromy matrix method, when carefully implemented, constitutes a significant advance over previous techniques for phase noise modeling in that it is based on a rigorous foundation that is uniformly applicable to any kind of oscillator. Its widespread adoption has, however, been hampered by two practical disadvantages. The first concerns locating the eigenpair of the oscillatory mode. Inaccuracies that are inevitable in any numerical procedure, and particularly in time-domain integration, often corrupt the oscillatory-mode eigenvalue of 1 to the extent that it cannot be distinguished from other eigenvalues of the system that are close to 1. This is particularly true for many LC oscillators. In such situations, a potentially large number of candidate PPVs are typically found and one chosen using heuristics, a process that is inconvenient and not entirely reliable.

Further, the monodromy matrix technique is inherently a time-domain procedure, requiring as it does the implementation of reverse time-domain integration of an adjoint system defined by a series of linearized oscillator matrices. Implementation of these operations in frequency-domain simulators based on harmonic balance (HB) can be very inconvenient. Reverse integration is often unavailable even in existing time-domain simulators and may require significant changes to core simulation routines.

In this paper, we provide new computational procedures for the PPV that alleviate both these disadvantages. The key to the techniques is that they do not form the monodromy matrix. Instead, they reuse the frequency- or time-domain Jacobian matrices of the oscillator that are formed during steady-state computation. A single linear equation solution with the Jacobian matrix suffices to find the PPV unambiguously. This is possible because the new methods locate the correct PPV directly by embedding exact periodicity and an orthonormality condition implicitly into the one-step calculation.

No eigencalculation is involved, and even for very large systems, the linear solution can be performed efficiently using fast methods for steady-state calculation (e.g., [2], [7], and[9]). The methods are easy to implement in existing simulators, since they require only an extra linear solution of the same Jacobian matrix that is generated and solved at each Newton step of the steady-state calculation, whether by HB or time-domain methods like shooting. This computation is negligible compared to that for obtaining the steady state. Note that variants of the monodromy matrix method, which use iterative techniques for eigencalculations, can achieve similarly low computation; however, in addition to the implementation complexity of reverse integration, iterative eigencalculations can further increase ambiguity in the selection of the oscillatory-mode eigenvalue.

The new techniques inherit the accuracy properties of the underlying steady-state method used to generate the Jacobian matrices. In particular, the frequency-domain version fully exploits the inherent matrix conditioning and accuracy advantages of HB. Time-domain numerical integration errors that lead to ambiguous eigenvalues in the monodromy matrix method do not create any similar problem for the new methods, due to the orthogonality condition that is implicitly embedded. Even though accuracies in time-domain computations are typically lower than in frequency-domain ones, the results are usually more than adequate in the context of the circuit or application.

If perfect numerics and no discretization errors were possible, the proposed procedure as well as the monodromy matrix method would calculate the exact PPV, because eigenanalysis in the monodromy matrix method would identify the oscillatory-mode eigenvalue of exactly one uniquely. In the presence of discretization and finite–precision arithmetic, however, the monodromy matrix method is no longer able to identify the oscillatory eigenmode uniquely; it must therefore select from among a number of potential eigenvalue choices. One way to make this choice is to investigate which eigenvector is "nearest" to orthonormality with the tangent to the steady-state solution. However, in general there is no guarantee that any of the candidate eigenvectors will be appreciably more orthonormal than the others, leading to a potential breakdown of the monodromy matrix method. In contrast, the new procedure, based on a linear matrix solution, remains well-defined and constitutes an unambiguous procedure to determine the PPV. The accuracy of this procedure degrades in the same manner, and for the same causes, as that of the underlying steady-state computation. In this context, the ambiguity of the monodromy matrix procedure can be thought of as stemming from its not making full use of underlying structure in the PPV problem.

Proof of correctness of the new methods relies on a link, established in Section II, between the PPV and the null space of the oscillator's frequency- and time-domain steady-state Jacobians. In Section III, we apply the new methods to two LC oscillators (including an example from industry) and a ring oscillator.

II. Relationship of the PPV $v_1(t)$ to the Oscillator's Steady-State Jacobian

We consider an orbitally stable oscillator with a single oscillation mode, described by the DAE system

$$\frac{\partial q(x)}{\partial t} + f(x) = 0. \tag{2}$$

We assume that this system has a known periodic solution $x_s(t)$. The linearization of (2) around the solution $x_s(t)$ is (e.g., [3] and[4])

$$\frac{d}{dt}\left(C(t)y(t)\right) + G(t)y(t) = 0. \tag{3}$$

$C(t)$ and $G(t)$ are periodic matrices. The rank m of $C(t)$ can be less than the system size n; m is assumed independent of t.

It can be shown (e.g., [3]) that, under reasonable assumptions, the state-transition matrix

$$\Phi(t,\, s) = U(t)D(t-s)V^T(s)C(s), \quad \text{with } D(t) = \operatorname{diag}(e^{\mu_1 t}, \ldots, e^{\mu_m t}, \underbrace{0, \ldots, 0}_{k=n-m}) \tag{4}$$

satisfies (3). $U(t)$ and $V(t)$ are periodic matrices of full rank satisfying the biorthogonality condition

$$V^T(t)C(t)U(t) = I_n = \begin{pmatrix} I_m & 0 \\ 0 & 0_k \end{pmatrix}. \tag{5}$$

$\mu_1, \ldots, \mu_m$ are the Floquet eigenvalues. Since the system has an oscillatory mode, one of these is zero, say $\mu_1 = 0$. The Floquet eigenvectors corresponding to this mode are the first

columns of $U(t)$ and $V(t)$, denoted by $u_1(t)$ and $v_1(t)$, respectively. It can be shown that $u_1(t)$ can be taken equal to $\dot{x}_s(t)$ without loss of generality [3] and computed easily from the known large-signal periodic solution. Our goal is to calculate the other oscillatory-mode Floquet eigenvector, $v_1(t)$.

It can be easily verified that the adjoint of (3), defined by

$$C^T(t)\frac{d}{dt}y(t) - G^T(t)y(t) = 0 \tag{6}$$

has the state-transition matrix

$$\Psi(t,\, s) = V(t)D(s-t)U^T(s)C^T(s) \tag{7}$$

which satisfies (6).

Before proceeding to connections with steady-state matrices, we establish the following two results (proofs are given in the Appendixes I and II):

Lemma II.1:

$$\begin{aligned} u_1(t) &= U(t)e_1 \text{ satisfies (3)} \\ v_1(t) &= V(t)e_1 \text{ satisfies (6)} \end{aligned} \tag{8}$$

where e_1 is the first unit vector, corresponding to $\mu_1 = 0$.

Lemma II.2:

$$\begin{aligned} M &= \left[\dot{V}^T(t)C(t) - V^T(t)G(t)\right]U(t)I_m \\ &= I_m\left[\dot{V}^T(t)C(t) - V^T(t)G(t)\right]U(t) \\ &\quad \text{where } M = \operatorname{diag}(\mu_1, \ldots, \mu_m, 0, \ldots, 0). \end{aligned} \tag{9}$$

A. Frequency-Domain Computations

Frequency-domain computations are natural for many applications, e.g., mildly nonlinear RF system components. We cast and apply (9) using frequency-domain quantities to establish a connection with HB.

We first develop some useful algebra involving Toeplitz matrices of Fourier components.

Definition II.1: Given any T-periodic vector or matrix $A(t)$, we denote its Fourier components by A_i, i.e.,

$$A(t) = \sum_i A_i e^{ji\omega_0 t}, \qquad \omega_0 = \frac{2\pi}{T}. \tag{10}$$

Definition II.2: Given any vector or matrix $A(t)$, define the block vector of its Fourier components to be

$$\overset{\text{FD}}{\mathbb{V}}_{A(t)} = \begin{pmatrix} \vdots \\ A_2 \\ A_1 \\ A_0 \\ A_{-1} \\ A_{-2} \\ \vdots \end{pmatrix}. \tag{11}$$

Definition II.3: Given any matrix or vector $A(t)$, define the block-Toeplitz matrix of its Fourier components to be

$$\mathbb{T}_{A(t)} = \begin{pmatrix} & \vdots & \vdots & \vdots & \vdots & \vdots & \\ \cdots & A_0 & A_1 & A_2 & A_3 & A_4 & \cdots \\ \cdots & A_{-1} & A_0 & A_1 & A_2 & A_3 & \cdots \\ \cdots & A_{-2} & A_{-1} & A_0 & A_1 & A_2 & \cdots \\ \cdots & A_{-3} & A_{-2} & A_{-1} & A_0 & A_1 & \cdots \\ \cdots & A_{-4} & A_{-3} & A_{-2} & A_{-1} & A_0 & \cdots \\ & \vdots & \vdots & \vdots & \vdots & \vdots & \end{pmatrix}. \tag{12}$$

Lemma II.3: If $X(t)$ and $Y(t)$ are T-periodic vectors or matrices, and $Z(t) = X(t)Y(t)$, then

$$\overset{\text{FD}}{\mathbb{V}}_{Z(t)} = \mathbb{T}_{X(t)}\overset{\text{FD}}{\mathbb{V}}_{Y(t)} \tag{13}$$

$$\mathbb{T}_{Z(t)} = \mathbb{T}_{X(t)}\mathbb{T}_{Y(t)}. \tag{14}$$

Lemma II.4: If $X(t)$ is a T-periodic vector or matrix, then

$$\overset{\text{FD}}{\mathbb{V}}_{\dot{X}(t)} = \overset{\text{FD}}{\Omega}\,\overset{\text{FD}}{\mathbb{V}}_{X(t)} \tag{15}$$

$$\mathbb{T}_{\dot{X}(t)} = \overset{\text{FD}}{\Omega}\,\mathbb{T}_{X(t)} - \mathbb{T}_{X(t)}\,\overset{\text{FD}}{\Omega} \tag{16}$$

where

$$\overset{\text{FD}}{\Omega} = j\omega_0 \begin{pmatrix} \ddots & & & & & & \\ & 2I_n & & & & & \\ & & I_n & & & & \\ & & & 0 & & & \\ & & & & -I_n & & \\ & & & & & -2I_n & \\ & & & & & & \ddots \end{pmatrix}. \tag{17}$$

We are now in a position to use the above definitions and lemmas. Applying (13) and (15) to (3), we obtain the linearized HB equations

$$\underbrace{\left[\overset{\text{FD}}{\Omega}\,\mathbb{T}_{C(t)} + \mathbb{T}_{G(t)}\right]}_{\overset{\text{HG}}{\mathbb{J}}}\overset{\text{FD}}{\mathbb{V}}_{y(t)} = 0. \tag{18}$$

Next, we state an important intermediate result:

Lemma II.5:

$$\left(\mathbb{T}_{V^T}\,\overset{\text{HB}}{\mathbb{J}}\,\mathbb{T}_U + \left[\mathbb{T}_M - \overset{\text{FD}}{\Omega}\right]\right)\mathbb{T}_{I_m} = 0 \tag{19}$$

and

$$\mathbb{T}_{I_m}\left(\mathbb{T}_{V^T}\,\overset{\text{HB}}{\mathbb{J}}\,\mathbb{T}_U + \left[\mathbb{T}_M - \overset{\text{FD}}{\Omega}\right]\right) = 0. \tag{20}$$

We concentrate on a single row of (20) by premultiplying by $\overset{\text{FD}}{\mathbb{V}}_{e_1}^T$, where e_1 is a unit vector (of size $m+k$) chosen to correspond to the oscillatory mode ($\mu_1 = 0$) of the system.

Theorem II.1:

$$\overset{\text{FD}}{\mathbb{V}}_{e_1}^T\,\mathbb{T}_{V^T}\,\overset{\text{HB}}{\mathbb{J}} = 0. \tag{21}$$

Remark II.1: From (21), we observe that $\mathbb{T}_{V^T}^T \overset{\text{FD}}{\mathbb{V}}_{e_1}$ [i.e., the vector of Fourier components of $v_1(t)$] is in the null space of J_{HB}^T, and that $\overset{\text{HB}}{\mathbb{J}}$ is singular.

Next, consider the augmented HB matrix

Definition II.4—Augmented HB Matrix for Oscillators:

$$\overset{\widetilde{\text{HB}}}{\mathbb{J}} = \begin{pmatrix} \overset{\text{HB}}{\mathbb{J}} & p \\ q^T & r \end{pmatrix}, \qquad \text{with} \quad \overset{\widetilde{\text{HB}}}{\mathbb{J}}^{-1} = \begin{pmatrix} A & b \\ l^T & d \end{pmatrix} \tag{22}$$

where p, q, b and l are column vectors, and r and d scalars.

$\overset{\widetilde{\text{HB}}}{\mathbb{J}}$ is the HB matrix augmented with a row and column, which are chosen to make it nonsingular. The following theorem establishes a simple means of computing the last row of its inverse.

Theorem II.2: If $p = \mathbb{T}_C \mathbb{T}_U \overset{\text{FD}}{\mathbb{V}}_{e_1}$ and $\overset{\widetilde{\text{HB}}}{\mathbb{J}}$ is nonsingular, then

$$l^T = \overset{\text{FD}}{\mathbb{V}}_{e_1}^T \mathbb{T}_{V^T}. \tag{23}$$

Remark II.2: $p = \mathbb{T}_C \mathbb{T}_U \overset{\text{FD}}{\mathbb{V}}_{e_1}$ is the vector of the Fourier coefficients of $C(t)\dot{x}_s(t)$, i.e., $p = \overset{\text{FD}}{\mathbb{V}}_{C(t)\dot{x}_s(t)}$.

Remark II.3: $l = \mathbb{T}_{V^T}^T \overset{\text{FD}}{\mathbb{V}}_{e_1}$ is the conjugated vector of the Fourier components of $v_1(t)$, i.e., $\overline{l} = \overset{\text{FD}}{\mathbb{V}}_{v_1(t)}$.

Corollary II.1: From (22), l is the solution of the system

$$\overset{\widetilde{\text{HB}}}{\mathbb{J}}^T \left[l^T, d\right]^T = [\ldots, 0, \ldots, 0, \ldots, 1]^T \tag{24}$$

hence, $\overline{l} = \overset{\text{FD}}{\mathbb{V}}_{v_1(t)}$ [i.e., the Fourier coefficients of $v_1(t)$] is the solution of

$$\overset{\widetilde{\text{HB}}}{\mathbb{J}}^* \left[\overline{l}^T, \overline{d}\right]^T = [\ldots, 0, \ldots, 0, \ldots, 1]^T. \tag{25}$$

Remark II.4: The augmented HB matrix $\overset{\widetilde{\text{HB}}}{\mathbb{J}}$, with $p = \mathbb{T}_C \mathbb{T}_U \overset{\text{FD}}{\mathbb{V}}_{e_1}$, arises naturally as the Jacobian matrix of the oscillator's steady-state equations augmented by a phase condition, with the frequency of oscillation as an additional unknown. Hence, from (25), the Fourier coefficients of $v_1(t)$ can be obtained from a single solution of the Hermitian of the augmented HB Jacobian of the oscillator, with right-hand side equal to a unit vector with value 1 in the phase condition equation. By exploiting circulant approximations to $\overset{\text{HB}}{\mathbb{J}}$ and applying iterative linear methods to solve (24), this computation becomes approximately linear in the system size.

We note that the accuracy of the calculation (25) is dominated primarily by the smallest of the nonoscillatory eigenvalues $\mu_2, \ldots, \mu_m$.[3] For high-Q oscillators, some of these eigenvalues can be very close to zero themselves. Since finding the steady-state solution of the oscillator is itself dependent on accurate solutions with the augmented HB matrix, it is to be expected that $v_1(t)$ will also be found to a similarly acceptable accuracy. This indicates that the main issue in calculating $v_1(t)$ by (25) is the accurate formation of, and solution with, the augmented HB matrix—a task that has already been accomplished during steady-state solution.[4]

Direct approaches to calculating $v_1(t)$, based on finding the 1-eigenpair of the system's state-transition or monodromy matrix, do not exploit the accuracy of the steady-state calculation to the same extent as (25). In the absence of a periodicity condition, transient integration errors can accumulate in computing the monodromy matrix, causing the oscillatory eigenvalue to become numerically indistinguishable from other eigenvalues close to 1. Hence, several eigenvectors corresponding to multiple eigenvalues close to 1 often need to be found, followed by subsequent selection of v_1 using the criterion of orthogonality with $C(t)\dot{x}_s(t)$. This orthogonality criterion is effectively embedded into (25), due to augmentation with p; as a result, calculation of multiple eigenvectors and subsequent selection is eliminated.

B. Time-Domain Computations

Time-domain computations are useful for systems with strong nonlinearities, such as ring oscillators. We first establish some notation.

Definition II.5: Denote by $\{t_0, \ldots, t_{N-1}\}$ a set of N ordered sample points of the interval $[0, T)$.

Definition II.6: Given any T-periodic vector or matrix $A(t)$, define

$$\overset{\text{TD}}{\mathbb{V}}_{A(t)} = \begin{pmatrix} A(t_0) \\ A(t_1) \\ \vdots \\ A(t_{N-1}) \end{pmatrix}. \tag{26}$$

Definition II.7: Given any T-periodic matrix or vector $A(t)$, define the block-diagonal matrix of its samples to be

$$\mathbb{D}_{A(t)} = \begin{pmatrix} A(t_0) & & & \\ & A(t_1) & & \\ & & \ddots & \\ & & & A(t_{N-1}) \end{pmatrix}. \tag{27}$$

Lemma II.6: If $X(t)$ and $Y(t)$ are T-periodic vectors or matrices, and $Z(t) = X(t)Y(t)$, then

$$\overset{\text{TD}}{\mathbb{V}}_{Z(t)} = \mathbb{D}_{X(t)} \overset{\text{TD}}{\mathbb{V}}_{Y(t)} \tag{28}$$

$$\mathbb{D}_{Z(t)} = \mathbb{D}_{X(t)} \mathbb{D}_{Y(t)}. \tag{29}$$

Proof: Follows directly from definition of $\overset{\text{TD}}{\mathbb{V}}$ and $\mathbb{D}$. ■

Lemma II.7: If $X(t)$ is a T-periodic vector or matrix, then

$$\overset{\text{TD}}{\mathbb{V}}_{\dot{X}(t)} = \overset{\text{TD}}{\Omega} \overset{\text{TD}}{\mathbb{V}}_{X(t)} \tag{30}$$

[3]The $\mu_1 = 0$ eigenvalue of the nonaugmented HB Jacobian is shifted to a nonzero value by the augmentation, resulting in a nonsingular augmented HB Jacobian.

[4]Note that all matrix computations are performed not with infinite matrices, but with *finite-dimensional circulant* approximations that arise naturally in fast HB algorithms. See, e.g., [8] for details.

where $\overset{\text{TD}}{\Omega}$ is a time-domain matrix that approximates differentiation, corresponding to a linear multistep formula. For example, $\overset{\text{TD}}{\Omega}$ for the Backward Euler method is

$$\overset{\text{TD}}{\Omega}_{\text{BE}} = \begin{pmatrix} (T-t_{N-1})I_n & & & \\ & (t_1-t_0)I_n & & \\ & & \ddots & \\ & & & (t_{N-1}-t_{N-2})I_n \end{pmatrix}^{-1} \cdot \begin{pmatrix} I_n & & & -I_n \\ -I_n & I_n & & \\ & \ddots & \ddots & \\ & & -I_n & I_n \end{pmatrix}.$$

Proof: Follows directly from the definitions of $\overset{\text{TD}}{\mathbb{V}}$ and $\overset{\text{TD}}{\Omega}$ and linear multistep formulas for differentiation. ■

We now establish the time-domain analog of (21)

Theorem II.3:

$$\underbrace{\left[\overset{\text{TD}}{\Omega}\,\mathbb{D}_{C(t)} + \mathbb{D}_{G(t)}\right]}_{\overset{\text{TD}}{\mathbb{J}_f}} \overset{\text{TD}}{\mathbb{V}}_{u_1(t)} = 0 \tag{31}$$

$$\underbrace{\left[\mathbb{D}_{C^T(t)}\,\overset{\text{TD}}{\Omega} - \mathbb{D}_{G^T(t)}\right]}_{\overset{\text{TD}}{\mathbb{J}_r}} \overset{\text{TD}}{\mathbb{V}}_{v_1(t)} = 0. \tag{32}$$

$\overset{\text{TD}}{\mathbb{J}_f}$ and $\overset{\text{TD}}{\mathbb{J}_r}$ are the forward and reverse time–domain Jacobian matrices, respectively. Next, consider the augmented Jacobian.

Definition II.8:

$$\overset{\widetilde{\text{TD}}}{\mathbb{J}_r} = \begin{pmatrix} \overset{\text{TD}}{\mathbb{J}_r} & p \\ q^T & r \end{pmatrix} \tag{33}$$

where p and q are column vectors and r is a scalar. $\overset{\widetilde{\text{TD}}}{\mathbb{J}_r}$ is the reverse time-domain Jacobian matrix augmented with a row and column, chosen to make it nonsingular.

Solving the following augmented Jacobian system results directly in the PPV $v_1(t)$

Theorem II.4: If $q = \overset{\text{TD}}{\mathbb{V}}_{(C(t)u_1(t))} = \mathbb{D}_C\mathbb{D}_U\overset{\text{TD}}{\mathbb{V}}_{e_1}$ and $\overset{\widetilde{\text{TD}}}{\mathbb{J}_r}$ is nonsingular,

$$\overset{\widetilde{\text{TD}}}{\mathbb{J}_r}\begin{pmatrix} x \\ y \end{pmatrix} = \begin{pmatrix} 0 \\ N \end{pmatrix} \tag{34}$$

has solution $x = \overset{\text{TD}}{\mathbb{V}}_{v_1(t)}$, $y = 0$.

As in the frequency-domain case, the equation system (34) can be solved efficiently with iterative methods, as a final step after solving the time-domain steady-state equations of the system.

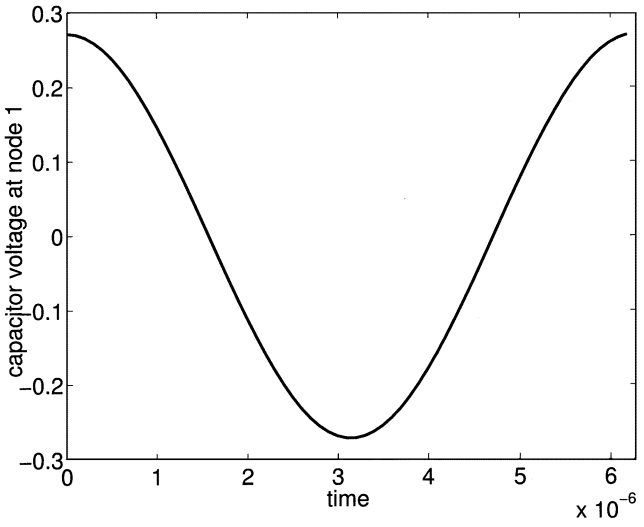

Fig. 2. Oscillator steady-state: voltage at capacitor.

III. Evaluation of the New Technique

In this section, we apply the time- and frequency-domain methods presented above to three oscillators. The first is an LC oscillator from Motorola. The remaining two examples (another LC oscillator and a three-stage ring oscillator) are provided with full details of the differential equations, to facilitate reproduction and verification of our results.

A. 160-kHz Motorola LC Oscillator

To evaluate the new method, it was compared against the established method that uses monodromy matrix eigendecomposition. The steady-state of a tank–circuit-based oscillator was computed using HB with $m = 31$ harmonics, resulting in $N = 63$ distinct frequency components. The frequency of oscillation f_0 was 159 154.853 364 298 Hz. The time-domain voltage waveform at the tank capacitor is shown in Fig. 2.

The PPV $v_1(t)$ was first determined through the time-domain monodromy matrix by computing its 1-eigenpair using iterative linear methods followed by manual selection from among candidate eigenpairs. The eigenvector thus obtained was then used as an initial condition for a transient simulation of the adjoint system, using a time–step corresponding to an oversampling factor of 4 (i.e., $4N$ timepoints) to limit accuracy loss from linear multistep formulae for DAE solution. The result of this transient simulation, after normalization, is the conventionally computed PPV. We refer to as $v_{1m}(t)$.

The new method described above simply computes the system (25) directly from the oscillator's HB Jacobian, with a single iterative linear solve. No oversampling is used by the method. The PPV obtained in this manner is denoted by $v_{1d}(t)$.

Fig. 3 depicts the components of $v_{1d}(t)$ (solid red line) and $v_{1m}(t)$ (black $\times$ marks) corresponding to the capacitor node. It can be seen that the PPV waveforms produced by the two methods are visually indistinguishable from each other. A more critical assessment of the two methods can be

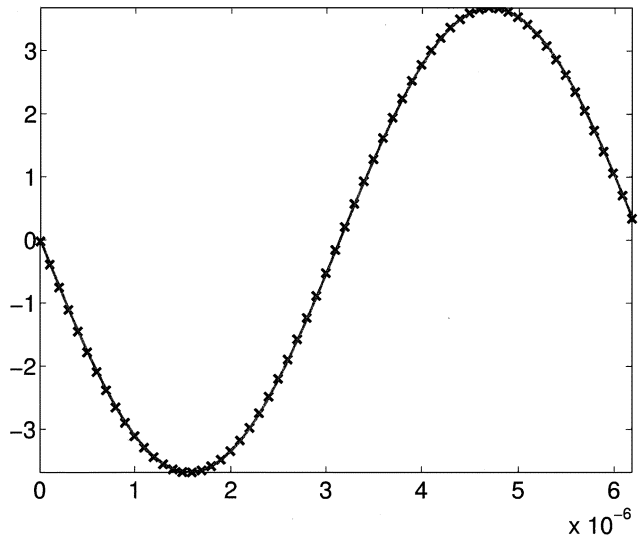

Fig. 3. Capacitor node of PPVs v_{1d} and v_{1m}.

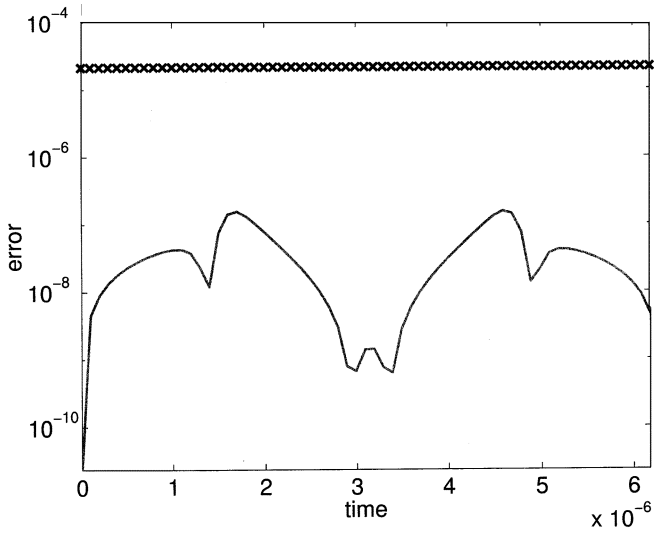

Fig. 4. Errors in the PPV obtained using the monodromy and new methods.

made using the fact that $u_1^T(t)v_1(t) \equiv 1$.[5] We plot the error $\epsilon_d(t) = |u_1^T(t)v_{1d}(t) - 1|$ versus $\epsilon_m(t) = |u_1^T(t)v_{1m}(t) - 1|$ in Fig. 4. The solid line indicates $\epsilon_d(t)$, the error of the new method, while the $\times$ marks indicate $\epsilon_m(t)$. The new method is about two orders of magnitude more accurate than monodromy matrix eigendecomposition, despite the $4\times$ oversampling used by the latter method.

B. 900 MHz, $Q = 4$ $\tanh$-Based LC Oscillator

The new techniques were also applied to an *LC* oscillator described by the following differential equations:

$$C\frac{d}{dt}v(t) = \frac{v(t)}{R} + i(t) + S\tanh\left(\frac{G_n}{S}v(t)\right)$$
$$L\frac{d}{dt}i(t) = -v(t). \tag{35}$$

[5]See, e.g., [5]. Note that $u_1(t)$ defined in (8) is identical to $p(t) = \overset{\text{FD}}{\mathbb{V}}_{C(t)\dot{x}_s(t)}$.

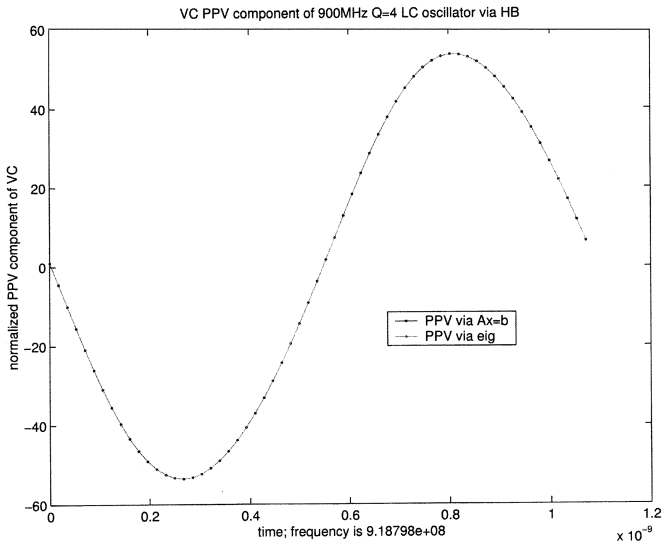

Fig. 5. $v(t)$ PPV component via HB, 900 MHz oscillator.

In the above equations, L, C, and R correspond to the inductance, capacitance, and resistance of an *LCR* tank circuit. S and G_n capture essential parameters of the negative-resistance nonlinearity that enables oscillations: RS corresponds roughly to the power–supply rail voltage, while G_n is the maximum (negative) conductance of the negative-resistance circuit. The circuit exhibits autonomous oscillations when $-G_n > 1/R$.

The circuit was simulated with the following parameters:

$$\begin{aligned} L &= 2\text{ nH} \\ C &= 15\text{ pF} \\ R &= 3\,\Omega \\ S &= \frac{1}{R} \\ G_n &= -\frac{1.01}{R}. \end{aligned} \tag{36}$$

These correspond to a natural frequency of about 918 MHz, a Q of about 4, a voltage swing of about 1 V, and relatively "linear" oscillation. These values are typical for on-chip RF oscillators with integrated spiral inductors.

The steady-state and the PPV of the oscillator were obtained independently using both HB and time-domain computations (i.e., the techniques described in Sections II-A and II-B) and compared, as described below. HB computations were carried out using 30 positive harmonic components for the steady-state, i.e., a total of 61 harmonic components including DC. The PPV waveforms were computed efficiently using the new technique, and compared with full eigendecomposition of the transposed (nonaugmented) HB matrix [refer to (21)]. The results are shown in Figs. 5 and 6 (the time-domain waveforms shown were obtained by post-processing results from the frequency-domain). The results from linear solution can be seen to be identical to those from explicit eigendecomposition. Furthermore, it can be seen from Fig. 6 that the result is accurate almost to machine precision.

Next, time-domain computations (based on FDTD using trapezoidal integration) were carried out. In order to make a fair comparison with HB, 61 equally spaced timepoints were

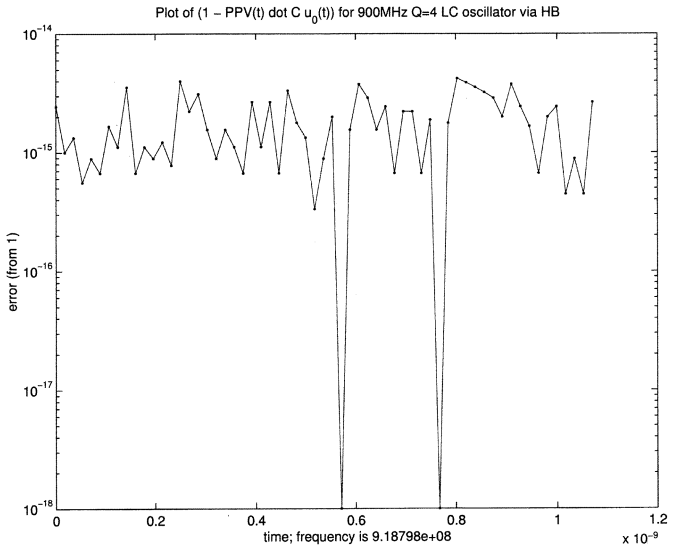

Fig. 6. Error in PPV orthogonality condition (HB), 900 MHz oscillator.

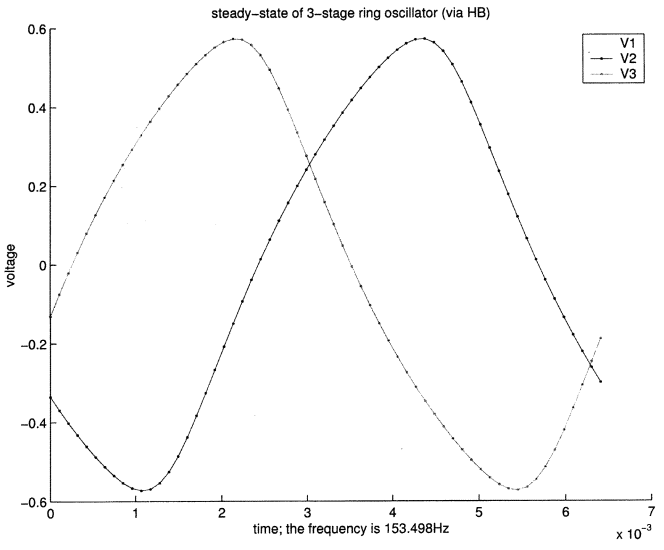

Fig. 7. Steady-state waveform via HB, ring oscillator.

used. There were small differences in the solutions compared to those from HB above, including in the oscillation frequency (918.798 MHz versus 917.986 MHz). The results from FDTD were less accurate (though still perfectly acceptable) than from HB. The reason for this is that the HB equations are exact for the fundamental Fourier component, the dominant mode of operation for this circuit; in particular, numerical differention in HB is exact. Any time-domain method based on linear multistep integration formulae, in contrast, inevitably approximates the differention operation.

C. Three-Stage Ring Oscillator

The proposed methods were also used to analyze a three-ring oscillator described by the following differential equations:

$$C\frac{d}{dt}v_1(t) = v_1 - \frac{\tanh(G_m v_3(t))}{R}$$
$$C\frac{d}{dt}v_2(t) = v_2 - \frac{\tanh(G_m v_1(t))}{R}$$
$$C\frac{d}{dt}v_3(t) = v_3 - \frac{\tanh(G_m v_2(t))}{R}. \quad (37)$$

The circuit was simulated with the following parameters:

$$C = 2\ \mu\text{F} \quad R = 1\ \text{k}\Omega \quad G_m = -5. \quad (38)$$

These parameters result in an oscillation frequency of about 153 Hz and a peak-to-peak swing of about 1.2 V.

HB computations were carried out using 30 positive harmonic components for the steady-state, i.e., a total of 61 harmonic components including dc. The results are shown in Figs. 7–9. All time-domain waveforms were obtained by post-processing results from the frequency-domain. The results from linear solution can be seen to be identical to those from explicit eigendecomposition. The PPV orthogonality error is quite low at about -140 dB (Fig. 9).

Time-domain computations (based on FDTD using trapezoidal integration) were carried out with 61 equally-spaced timepoints. As with the *LC* oscillator above, the results are not

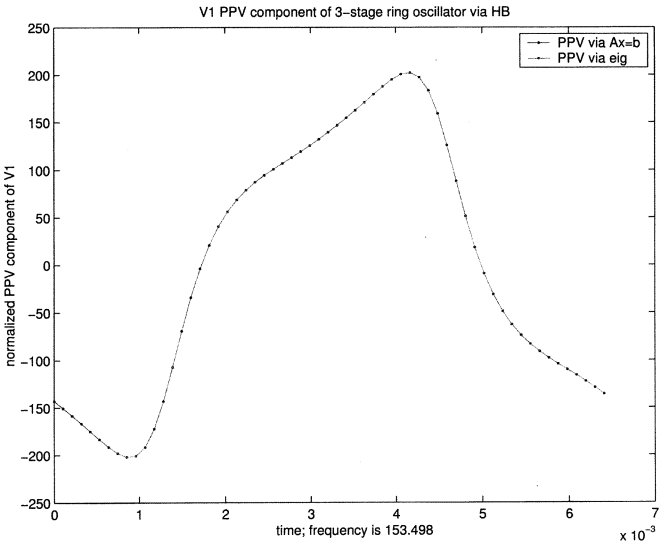

Fig. 8. v_1 PPV component via HB (time-domain), ring oscillator.

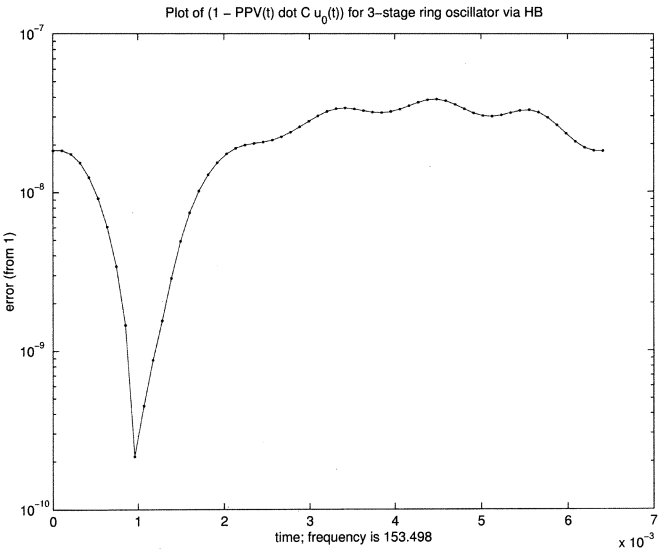

Fig. 9. Orthogonality error in PPV via HB, ring oscillator.

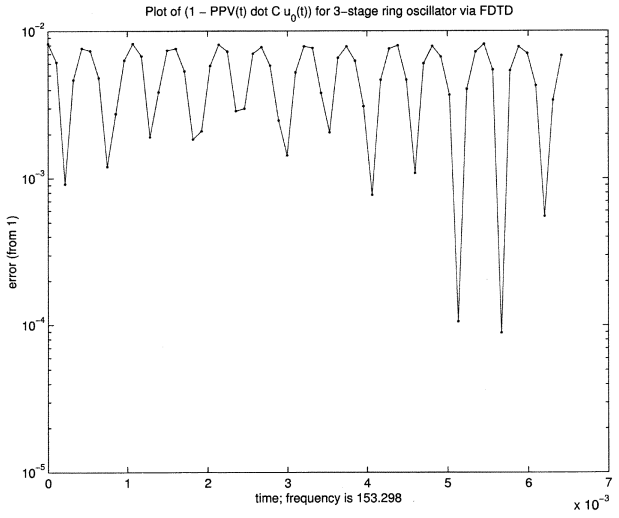

Fig. 10. Orthogonality error in PPV via FDTD, ring oscillator.

exactly identical to those from HB. In particular, the orthogonality condition error (shown in Fig. 10) at about -40 dB is considerably worse than that using HB computations. This error may be acceptable in many situations; when it is not (and HB solution is not feasible), more timepoints and higher order integration formulas can be used for greater accuracy.

Appendix I
Matrix Notation for Jacobians

Lemma II.3: If $X(t)$ and $Y(t)$ are T-periodic vectors or matrices, and $Z(t) = X(t)Y(t)$, then

$$\overset{\text{FD}}{\mathbb{V}}_{Z(t)} = \mathbb{T}_{X(t)} \overset{\text{FD}}{\mathbb{V}}_{Y(t)} \tag{39}$$

$$\mathbb{T}_{Z(t)} = \mathbb{T}_{X(t)} \mathbb{T}_{Y(t)}. \tag{40}$$

Proof: From definition,

$$\sum_i Z_i e^{ji\omega_0 t} = \sum_{k,l} X_k Y_l e^{j(k+l)\omega_0 t}$$

$$\Rightarrow Z_i = \sum_l X_{i-l} Y_l. \tag{41}$$

Equation (13) follows directly.

Next, we rewrite (41) as

$$Z_{i+k} = \sum_l X_{i-(l-k)} Y_l = \sum_{l'=l-k} X_{i-l'} Y_{l'+k}. \tag{42}$$

Equation (42) yields the kth block–column of $\mathbb{T}_{Z(t)}$, hence, (14) follows. ∎

Lemma II.4: If $X(t)$ is a T-periodic vector or matrix, then

$$\overset{\text{FD}}{\mathbb{V}}_{\dot{X}(t)} = \overset{\text{FD}}{\Omega}\, \overset{\text{FD}}{\mathbb{V}}_{X(t)} \tag{43}$$

$$\mathbb{T}_{\dot{X}(t)} = \overset{\text{FD}}{\Omega}\, \mathbb{T}_{X(t)} - \mathbb{T}_{X(t)}\, \overset{\text{FD}}{\Omega} \tag{44}$$

where

$$\overset{\text{FD}}{\Omega} = j\omega_0 \begin{pmatrix} \ddots & & & & & & \\ & 2I_n & & & & & \\ & & I_n & & & & \\ & & & 0 & & & \\ & & & & -I_n & & \\ & & & & & -2I_n & \\ & & & & & & \ddots \end{pmatrix}. \tag{45}$$

Proof: Using

$$\dot{X}(t) = \sum_i ji\omega_0 X_i e^{j\omega_0 it}$$

(15) and (16) may be verified directly. ∎

Lemma II.6: If $X(t)$ and $Y(t)$ are T-periodic vectors or matrices, and $Z(t) = X(t)Y(t)$, then

$$\overset{\text{TD}}{\mathbb{V}}_{Z(t)} = \mathbb{D}_{X(t)} \overset{\text{TD}}{\mathbb{V}}_{Y(t)} \tag{46}$$

$$\mathbb{D}_{Z(t)} = \mathbb{D}_{X(t)} \mathbb{D}_{Y(t)}. \tag{47}$$

Proof: Follows directly from definition of $\overset{\text{TD}}{\mathbb{V}}$ and $\mathbb{D}$. ∎

Lemma II.7: If $X(t)$ is a T-periodic vector or matrix, then

$$\overset{\text{TD}}{\mathbb{V}}_{\dot{X}(t)} = \overset{\text{TD}}{\Omega}\, \overset{\text{TD}}{\mathbb{V}}_{X(t)} \tag{48}$$

where $\overset{\text{TD}}{\Omega}$ is a time-domain matrix that approximates differentiation, corresponding to a linear multistep formula. For example, $\overset{\text{TD}}{\Omega}$ for the Backward Euler method is

$$\overset{\text{TD}}{\Omega}_{\text{BE}} = \begin{pmatrix} (T - t_{N-1})\, I_n & & & \\ & (t_1 - t_0) I_n & & \\ & & \ddots & \\ & & & (t_{N-1} - t_{N-2})\, I_n \end{pmatrix}^{-1} \cdot \begin{pmatrix} I_n & & & -I_n \\ -I_n & I_n & & \\ & \ddots & \ddots & \\ & & -I_n & I_n \end{pmatrix}.$$

Proof: Follows directly from the definitions of $\overset{\text{TD}}{\mathbb{V}}$ and $\overset{\text{TD}}{\Omega}$ and linear multistep formulas for differentiation. ∎

Appendix II
Proofs of Theorems and Lemmas

Lemma II.1:

$$u_1(t) = U(t)e_1 \text{ satisfies (3)}$$

$$v_1(t) = V(t)e_1 \text{ satisfies (6)} \tag{49}$$

where e_1 is the first unit vector, corresponding to $\mu_1 = 0$.

Proof: By definition of the state-transition matrix, $\Phi(t, s)u_1(s)$ satisfies (3) with initial condition $u_1(s)$ at $t = s$. Now,

$$\begin{aligned} \Phi(t, s)u_1(s) &= U(t)D(t-s)V^T(s)C(s)U(s)e_1 \\ &= U(t)D(t-s)I_m e_1 = U(t)D(t-s)e_1 \\ &= U(t)e^{\mu_1(t-s)}e_1 = u_1(t). \end{aligned}$$

The proof for $v_1(t)$ proceeds similarly, using $\Psi(t, s)$ and (6). ∎

Lemma II.2:

$$M = \left[\dot{V}^T(t)C(t) - V^T(t)G(t)\right]U(t)I_m$$
$$= I_m\left[\dot{V}^T(t)C(t) - V^T(t)G(t)\right]U(t)$$
$$\text{where } M = \text{diag}(\mu_1, \ldots, \mu_m, 0, \ldots, 0). \quad (50)$$

Proof:

$C(t)\Phi(t, s) = C(t)U(t)D(t-s)V^T(s)C(s)$ [from (4)]

$\Rightarrow V^T(t)C(t)\Phi(t, s) = I_m D(t-s)V^T(s)C(s)$ [using (5)]

$\Rightarrow \dfrac{d}{dt}\left[V^T(t)C(t)\Phi(t, s)\right] = I_m M D(t-s)V^T(s)C(s).$

Also,

$$\frac{d}{dt}\left[V^t(t)C(t)\Phi(t, s)\right]$$
$$= \dot{V}^T(t)C(t)\Phi(t, s) + V^T(t)\frac{d}{dt}\left[C(t)\Phi(t, s)\right]$$
$$= \dot{V}^T(t)C(t)\Phi(t, s) - V^T(t)G(t)\Phi(t, s) \text{ [using (3)]}.$$

Hence,

$$I_m M D(t-s)V^T(s)C(s)$$
$$= \left[\dot{V}^T(t)C(t) - V^T(t)G(t)\right]\Phi(t, s)$$
$$= \left[\dot{V}^T(t)C(t) - V^T(t)G(t)\right]U(t)D(t-s)V^T(s)C(s).$$

Postmultiplying by $U(s)$ and applying (5), we obtain

$$I_m M D(t-s)I_m = \left[\dot{V}^T(t)C(t) - V^T(t)G(t)\right]U(t)D(t-s)I_m.$$

Setting $s = t$ and using the diagonal properties of M and $D(\cdot)$, we obtain

$$M = \left[\dot{V}^T(t)C(t) - V^T(t)G(t)\right]U(t)I_m.$$

From the definition of $\Psi(t, s)$, we have

$$\frac{d}{dt}\Psi(t, s) = \left[\dot{V}(t) - V(t)M\right]D(s-t)U^T(s)C^T(s).$$

Using (6), we obtain

$$\left\{C^T(t)\left[\dot{V}(t) - V(t)M\right] - G^T(t)V(t)\right\}$$
$$\cdot D(s-t)U^T(s)C^T(s) = 0$$
$$\Rightarrow C(s)U(s)D(s-t)$$
$$\cdot \left\{\left[\dot{V}^T(t) - MV^T(t)\right]C(t) - V^T(t)G(t)\right\} = 0.$$

Premultiplying by $V^T(s)$ and setting $s = t$, we obtain

$$I_m\left\{\left[\dot{V}^T(t) - MV^T(t)\right]C(t) - V^T(t)G(t)\right\} = 0.$$

Postmultiplying by $U(t)$, we have

$$I_m\left[\dot{V}^T(t)C(t)U(t) - V^T(t)G(t)U(t)\right] = I_m M I_m = M.$$

■

Lemma II.5:

$$\left(\mathbb{T}_{V^T}\overset{\text{HB}}{\mathbb{J}}\mathbb{T}_U + \left[\mathbb{T}_M - \overset{\text{FD}}{\Omega}\right]\right)\mathbb{T}_{I_m} = 0 \quad (51)$$

and

$$\mathbb{T}_{I_m}\left(\mathbb{T}_{V^T}\overset{\text{HB}}{\mathbb{J}}\mathbb{T}_U + \left[\mathbb{T}_M - \overset{\text{FD}}{\Omega}\right]\right) = 0. \quad (52)$$

Proof: We first note that, from (14) and (5),

$$\mathbb{T}_{V^T}\mathbb{T}_C\mathbb{T}_U = \mathbb{T}_{I_m}. \quad (53)$$

Applying (14) and (16) to (9), we obtain

$$\mathbb{T}_M = \left[\left(\overset{\text{FD}}{\Omega}\mathbb{T}_{V^T} - \mathbb{T}_{V^T}\overset{\text{FD}}{\Omega}\right)\mathbb{T}_C - \mathbb{T}_{V^T}\mathbb{T}_G\right]\mathbb{T}_U\mathbb{T}_{I_m}$$
$$= \left[\overset{\text{FD}}{\Omega} - \mathbb{T}_{V^T}\overset{\text{HB}}{\mathbb{J}}\mathbb{T}_U\right]\mathbb{T}_{I_m} \text{ [using (53) and (18)]}.$$

Similarly,

$$\mathbb{T}_M = \mathbb{T}_{I_m}\left[\overset{\text{FD}}{\Omega} - \mathbb{T}_{V^T}\overset{\text{HB}}{\mathbb{J}}\mathbb{T}_U\right].$$

From the diagonal structure of M and I_m, we have $\mathbb{T}_M = \mathbb{T}_M\mathbb{T}_{I_m} = \mathbb{T}_{I_m}\mathbb{T}_M$, and the assertions follow. ■

Theorem II.1:

$$\overset{\text{FD}}{\mathbb{V}}{}_{e_1}^T\mathbb{T}_{V^T}\overset{\text{HB}}{\mathbb{J}} = 0. \quad (54)$$

Proof: Premultiplying (20) by $\mathbb{T}_{e_1}^T$ and noting that $\overset{\text{FD}}{\mathbb{V}}{}_{e_1}^T\mathbb{T}_{I_m} = \overset{\text{FD}}{\mathbb{V}}{}_{e_1}^T$, we have

$$\overset{\text{FD}}{\mathbb{V}}{}_{e_1}^T\mathbb{T}_{V^T}\overset{\text{HB}}{\mathbb{J}} = \overset{\text{FD}}{\mathbb{V}}{}_{e_1}^T\left[\overset{\text{FD}}{\Omega} - \mathbb{T}_M\right]\mathbb{T}_U^{-1}.$$

From the definition of $\overset{\text{FD}}{\Omega}$ and using $\mu_1 = 0$, we have $\overset{\text{FD}}{\mathbb{V}}{}_{e_1}^T\overset{\text{FD}}{\Omega} = 0$ and $\overset{\text{FD}}{\mathbb{V}}{}_{e_1}^T\mathbb{T}_M = 0$, proving the result. ■

Theorem II.2: If $p = \mathbb{T}_C\mathbb{T}_U\overset{\text{FD}}{\mathbb{V}}_{e_1}$ and $\widetilde{\overset{\text{HB}}{\mathbb{J}}}$ is nonsingular, then

$$l^T = \overset{\text{FD}}{\mathbb{V}}{}_{e_1}^T\mathbb{T}_{V^T}. \quad (55)$$

Proof: From (22) and $p = \mathbb{T}_C\mathbb{T}_U\overset{\text{FD}}{\mathbb{V}}_{e_1}$, we have

$$\overset{\text{HB}}{\mathbb{J}}A + \mathbb{T}_C\mathbb{T}_U\overset{\text{FD}}{\mathbb{V}}_{e_1}l^T = I$$
$$\Rightarrow \mathbb{T}_{V^T}\overset{\text{HB}}{\mathbb{J}}A + \mathbb{T}_{V^T}\mathbb{T}_C\mathbb{T}_U\overset{\text{FD}}{\mathbb{V}}_{e_1}l^T = \mathbb{T}_{V^T}$$
$$\Rightarrow \mathbb{T}_{V^T}\overset{\text{HB}}{\mathbb{J}}A + \overset{\text{FD}}{\mathbb{V}}_{e_1}l^T = \mathbb{T}_{V^T}$$
$$\Rightarrow \overset{\text{FD}}{\mathbb{V}}{}_{e_1}^T\mathbb{T}_{V^T}\overset{\text{HB}}{\mathbb{J}}A + \overset{\text{FD}}{\mathbb{V}}{}_{e_1}^T\overset{\text{FD}}{\mathbb{V}}_{e_1}l^T = \overset{\text{FD}}{\mathbb{V}}{}_{e_1}^T\mathbb{T}_{V^T}$$
$$\Rightarrow l^T = \overset{\text{FD}}{\mathbb{V}}{}_{e_1}^T\mathbb{T}_{V^T} \text{ [using (21)]}.$$

■

Theorem II.3:

$$\underbrace{\left[\overset{\text{TD}}{\Omega}\mathbb{D}_{C(t)} + \mathbb{D}_{G(t)}\right]}_{\overset{\text{TD}}{\mathbb{J}}_f}\overset{\text{TD}}{\mathbb{V}}_{u_1(t)} = 0 \quad (56)$$

$$\underbrace{\left[\mathbb{D}_{C^T(t)}\overset{\text{TD}}{\Omega} - \mathbb{D}_{G^T(t)}\right]}_{\overset{\text{TD}}{\mathbb{J}}_r}\overset{\text{TD}}{\mathbb{V}}_{v_1(t)} = 0. \quad (57)$$

Proof: The results follow from applying (28) and (30) to (3) and (6) and using (8). ■

Theorem II.4: If $q = \overset{\text{TD}}{\mathbb{V}}_{(C(t)u_1(t))} = \mathbb{D}_C\mathbb{D}_U \overset{\text{TD}}{\mathbb{V}}_{e_1}$ and $\overset{\widetilde{\text{TD}}}{\mathbb{J}}_r$ is nonsingular,

$$\overset{\widetilde{\text{TD}}}{\mathbb{J}}_r \begin{pmatrix} x \\ y \end{pmatrix} = \begin{pmatrix} 0 \\ N \end{pmatrix} \tag{58}$$

has solution $x = \overset{\text{TD}}{\mathbb{V}}_{v_1(t)}$, $y = 0$.

Proof: Because $\overset{\text{TD}}{\mathbb{J}}_r$ is nonsingular, (34) has a unique solution. We show that $x = \overset{\text{TD}}{\mathbb{V}}_{v_1(t)}$, $y = 0$ satisfies (34). We have

$$\overset{\text{TD}}{\mathbb{J}}_r x + py = 0$$
$$q^T x + ry = N.$$

From (32), $\overset{\text{TD}}{\mathbb{J}}_r x = 0$, hence the first equation is satisfied. Applying (28) to the transpose of (5), we have

$$\mathbb{D}_{U^T}\mathbb{D}_{C^T} \overset{\text{TD}}{\mathbb{V}}_V = \overset{\text{TD}}{\mathbb{V}}_{I_m}.$$

Since $x = \overset{\text{TD}}{\mathbb{V}}_{v_1(t)} = \overset{\text{TD}}{\mathbb{V}}_{V(t)}e_1$, we have

$$q^T x = \overset{\text{TD}}{\mathbb{V}}_{e_1}{}^T \mathbb{D}_{U^T}\mathbb{D}_{C^T} \overset{\text{TD}}{\mathbb{V}}_V e_1$$
$$= \overset{\text{TD}}{\mathbb{V}}_{e_1}{}^T \overset{\text{TD}}{\mathbb{V}}_{I_m} e_1 = \overset{\text{TD}}{\mathbb{V}}_{e_1}{}^T \overset{\text{TD}}{\mathbb{V}}_{e_1} = N.$$

Hence, the second equation is also satisfied, and the result is proved. ■

ACKNOWLEDGMENT

The authors would like to acknowledge K. Gullapalli (Motorola Inc.) for providing the first test oscillator circuit, its steady-state solution, and $v_1(t)$ computed using monodromy matrix methods.

REFERENCES

[1] A. Demir, D. Long, and J. Roychowdhury, "Computing phase noise eigenfunctions directly from steady-state Jacobian matrices," in *Proc. ICCAD*, Nov. 2000, pp. 283–288.

[2] D. Long *et al.*, "Full chip harmonic balance," in *Proc. IEEE CICC*, May 1997, pp. 379–382.

[3] A. Demir, "Phase noise in oscillators: DAE's and colored noise sources," in *Proc. ICCAD*, 1998, pp. 170–177.

[4] A. Demir, A. Mehrotra, and J. Roychowdhury, "Phase noise in oscillators: A unifying theory and numerical methods for characterization," *IEEE Trans. Circuits Syst. I*, vol. 47, pp. 655–674, May 2000.

[5] M. Farkas, *Periodic Motions*. Berlin, Germany: Springer-Verlag, 1994.

[6] W. P. Robins, *Phase Noise in Signal Sources*. Stevenage, U.K.: Peregrinus, 1991.

[7] M. Rösch and K. J. Antreich, "Schnell stationäre simulation nichtlinearer schaltungen im frequenzbereich," *Archiv Elektronik Übertragungstechnik*, vol. 46, no. 3, pp. 168–176, 1992.

[8] J. Roychowdhury, D. Long, and P. Feldmann, "Cyclostationary noise analysis of large RF circuits with multitone excitations," *IEEE J. Solid-State Circuits*, vol. 33, pp. 324–336, Mar. 1998.

[9] R. Telichevesky, K. Kundert, and J. White, "Efficient steady-state analysis based on matrix-free Krylov subspace methods," in *Proc. IEEE DAC*, 1995, pp. 480–484.

Alper Demir (S'93–M'96) received the B.S. degree in electrical engineering from Bilkent University, Turkey, in 1991, and the M.S. and Ph.D. degrees in electrical engineering and computer sciences from the University of California, Berkeley in 1994 and 1997, respectively.

From May 1992 to January 1997, he worked as a Research and Teaching Assistant in the Electronics Research Laboratory and the Electrical Engineering and Computer Sciences at the University of California, Berkeley. He was with Motorola Inc., Summer 1995, and with Cadence Design Systems, Summer 1996. He joined the Research Division of Bell Laboratories, Lucent Technologies as a member of the technical staff in January 1997, where he has spent four years. He was with CeLight, a start-up in optical communications, from November 2000 to February 2002, where he was the Manager for Optical Telecommunications Systems Design. He is now an Assistant Professor in the Department of Electrical and Computer Engineering, Koç University, Istanbul, Turkey. His research work is on the fundamental theory and algorithms for design analysis, verification and design automation of electronic and opto-electronic discrete/integrated circuits and systems, with emphasis on analog/mixed-signal circuits, electromagnetic, wave propagation, nonlinear, time-varying, and noise phenomena in RF/wireless/high-speed/optical communications. The work he has done at Bell Labs and CeLight is the subject of eight patents. He has coauthored two books in the areas of nonlinear noise analysis and analog design methodologies.

Dr. Demir received the Regents Fellowship from the University of California, Berkeley, in 1991, and was selected to be an Honorary Fellow of the Scientific and Technical Research Council of Turkey (TÜBİTAK).

Jaijeet Roychowdhury (S'85–M'87) received the Bachelor's degree in electrical engineering from the Indian Institute of Technology, Kanpur, India in 1987, and the Ph.D. degree in electrical engineering and computer science from the University of California, Berkeley, in 1993.

He was with the CAD Lab, AT&T Bell Laboratories, Allentown, PA from 1993 to 1995. From 1995 to 2000, he was with the Communication Sciences Research Division, Lucent Bell Laboratories, Murray Hill, NJ. From 2000 to 2001, he was with CeLight, Inc., Silver Spring, MD, an optical networking startup. Since 2001, he has been with the Department of Electrical and Computer Engineering and the Digital Technology Center, University of Minnesota, Minneapolis. His professional interests include the design, analysis, and simulation of electronic, electrooptical, and mixed-domain systems, particularly for high-speed and high-frequency communications.

Dr. Roychowdhury received Distinguished and Best Paper Awards at ICCAD 1991, DAC 1997, ASP-DAC 1997, and ASP-DAC 1999, and was cited for Extraordinary Achievement by Bell Laboratories.